JOURNAL OF SPACECRAFT AND ROCKETS
Vol. 40, No. 2, March–April 2003

Optimal Control Law for Interplanetary Trajectories with Nonideal Solar Sail

Guido Colasurdo* and Lorenzo Casalino†
Politecnico di Torino, 10129 Turin, Italy

An indirect method is applied to minimize the trip time of interplanetary and escape missions using solar sails. A flat sail and specular reflection of the incident radiation is assumed. The theory of optimal control provides the equation that gives the optimal orientation of the sail at each point of the trajectory. An analytical solution can be obtained in the ideal case (unit reflectivity) when all of the incident radiation is specularly reflected. The equation is numerically solved when the incident radiation is partially absorbed (nonunit reflectivity). Once the reflectivity has been assumed, the optimal trajectory only depends on the sail characteristic acceleration. The optimization procedure has been used to estimate the performance of different missions; the influence of the sail reflectivity is in particular pointed out. Transfers to Mars and Mercury and escape from the solar system are presented.

Nomenclature

A	=	sail area
a	=	acceleration
a_c	=	characteristic acceleration
H	=	Hamiltonian
H'	=	function; see Eq. (10)
k_p	=	payload fraction
m	=	mass
p	=	radiation pressure
p_1	=	radiation pressure at 1 astronomical unit
r	=	radius
t	=	time
u	=	radial velocity
v	=	tangential velocity
α	=	sail angle
β	=	primer vector orientation angle
η	=	sail reflectivity
θ	=	right ascension
λ_x	=	adjoint variable corresponding to state variable x
$\boldsymbol{\lambda}_V$	=	primer vector
σ	=	sail areal density
ϕ	=	performance index

Subscripts

a	=	aphelion
f	=	final
min	=	minimum distance from the sun
p	=	perihelion
s	=	sail
t	=	target planet
u	=	radial direction
v	=	tangential direction
0	=	initial

Received 23 April 2002; revision received 5 December 2002; accepted for publication 12 December 2002.

*Professor, Dipartimento di Energetica, Corso Duca degli Abruzzi, 24. Associate Fellow AIAA.

†Associate Professor, Dipartimento di Energetica, Corso Duca degli Abruzzi, 24. Member AIAA.

Introduction

A SOLAR sail consists of a large surface of light and reflective material, for example, a metallized plastic film, supported by a suitable structure. Solar radiation pressure interacts with the sail and produces thrust. Propulsion by means of a solar sail does not require propellant, and the propulsion system is completely reusable. On the other hand, the thrust that can be provided is limited, and large sails are required to keep the trip time reasonable. In the case of an ideal sail, the maximum thrust per unit sail area is twice the radiation pressure, which is approximately 4.5 N/km^2 at 1 astronomical unit (AU) and varies with the inverse of the squared distance from the sun. The sail mass is the penalty which reduces the payload. NASA; the National Oceanic and Atmospheric Administration; the U.S. Department of Defense; the DLR, German Aerospace Research Center; and ESA are presently considering the solar sail in their technology development programs. According to the sail areal density, different missions can be performed, for example, missions to the interior planets, asteroid rendezvous, and missions to Mars and toward the exterior of the solar system.

The orientation of the solar sail relative to the sun-sail direction determines the thrust magnitude and direction. The magnitude is maximum when the sail is perpendicular to the radial direction and is reduced when the sail is rotated to obtain a tangential component of the thrust. Because of the low thrust, the spacecraft velocity is usually almost circular, and the radial component of the thrust is often useless to vary the spacecraft energy; a compromise between thrust magnitude and useful orientation must be sought, and a complex optimization problem arises. In the ideal case (specular reflection and unit reflectivity), the sail specularly reflects all of the incident radiation. Forward[1] has discussed the effects of the optical properties of realistic solar sails. In particular, part of the incident radiation is transmitted through the sail, part is reflected backward, that is, toward the sun, part is diffused, and part is absorbed and emitted from both sides of the sail. The properties of the sail influence the thrust magnitude and direction: The thrust magnitude decreases if the reflectivity is reduced, and a reduction of the sail reflectivity tends to tilt the thrust direction radially, in comparison to the ideal case.

The trajectory optimization of solar sails with unit reflectivity has been frequently addressed in the literature. Different kind of missions have been considered, and a short and rather incomplete list of references[2–8] is given here. Sauer[2] applied the theory of optimal control to calculate interplanetary trajectories for an ideal, perfectly reflecting sail. Wood et al.[3] have discussed minimum-time heliocentric transfers between the Earth's and Mars's orbits, which are assumed to be circular and coplanar. Subba Rao and Ramanan[4] have optimized the transfer between elliptical orbits of an ideal sail, by the use of the angular position as the independent variable. Sauer[5]

has recently presented three-dimensional optimal trajectories for escape from the solar system and solar polar missions. McInnes[6] has analyzed the optimal trajectories to Mars using the compound sail that promises better performance than the classical single-reflection sail. Nonideal sails have been rarely considered. Some peculiarities of the optimal trajectories for real flat sails are marginally presented by Sauer[7] in a paper where he compares different propulsion options to intercept Halley's comet. Cichan and Melton[8] presented a direct optimization method for a nonideal billowing sail that takes into account the finite dimension of the sun.

In the present paper, the theory of optimal control is applied to provide the optimal control law (i.e., the equation that gives the optimal orientation of the solar sail at each point of the trajectory) when the sail reflectivity is not unit and the absorbed radiation is eventually emitted in equal amounts from both sides of the sail. An analytical solution can be obtained in the case of unit reflectivity, whereas the equation that provides the optimal sail orientation is numerically solved for lower reflectivity. In the latter case, zero-thrust arcs may be necessary to avoid any adverse radial component of the sail thrust when the spacecraft moves toward the sun. The optimal trajectories of ideal and nonideal sails and the corresponding control laws are compared for missions toward either inner or outer planets and for the escape from the solar system, to estimate the penalty related to the nonunit reflectivity of the sail.

Equations of Motion

For the sake of simplicity, a flat sail is considered, and spacecraft motion in the ecliptic plane is also assumed. Coplanar circular orbits are assumed for the planets. The sail is hit by the solar radiation and reflects a fraction η of the incident radiation. The sail orientation angle α, which is the angle between the sail and the local horizon, or, equivalently, the angle between the sail outward normal and the radial direction (Fig. 1), is the problem control variable. Angle α is positive when the sail is rotated in accordance with the motion of the Earth on the ecliptic plane, which is assumed to be counterclockwise in Fig. 1; admissible values for α range from -90 to 90 deg. Specular reflection is supposed, and the angle between the reflected radiation and the sail-sun direction is 2α. The momentum flux, which is associated with the radiation, is the ratio of the power flux to the light speed. The change of radiation momentum produces the thrust on the sail, and the corresponding thrust density is the vectorial difference between the incident and reflected momentum flux. The acceleration of the sail, which is produced by the solar radiation in the radial and tangential directions, can be easily obtained:

$$a_u = pA\cos\alpha(1+\eta\cos 2\alpha)/m \tag{1}$$

$$a_v = pA\cos\alpha\eta\sin 2\alpha/m \tag{2}$$

where m is the spacecraft mass and p is the incident momentum flux (usually referred to as the solar radiation pressure), which is inversely proportional to the squared distance from the sun. The acceleration obtained when the sail is oriented normal to sunlight ($\alpha = 0$) at 1 AU, where the solar pressure is $p_1 = 4.55682$ N/km^2, is defined as the characteristic acceleration $a_c = 2p_1A/m$. Note that the present analysis is still valid if part of the solar radiation is either transmitted through the sail or reflected backward, but the radiation pressure and the sail reflectivity must be corrected taking the optical properties of the sail into account. On the contrary, different equations apply if a portion of the incident radiation is reflected diffusely or the absorbed energy is radiated in different amounts from the frontside and the backside of the sail.

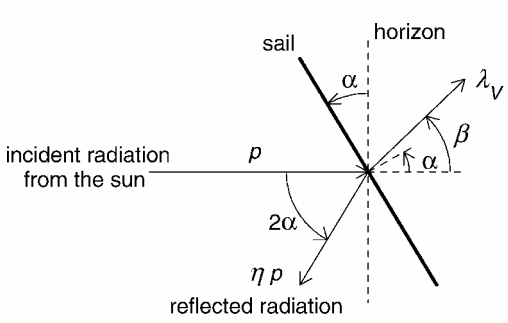

Fig. 1 Solar sail operation.

Throughout, the variables are normalized using the radius of Earth's orbit and the corresponding circular velocity as the reference values. When the sail position is expressed in polar coordinates (r and θ) and its velocity is expressed as components in the radial and tangential directions (u and v, respectively), the equations of motion are

$$\dot{r} = u \tag{3}$$

$$\dot{\theta} = v/r \tag{4}$$

$$\dot{u} = v^2/r - 1/r^2 + a_c\cos\alpha(1+\eta\cos 2\alpha)/(2r^2) \tag{5}$$

$$\dot{v} = -uv/r + a_c\cos\alpha\eta\sin 2\alpha/(2r^2) \tag{6}$$

where a_c is now the nondimensional characteristic acceleration.

Trajectory Optimization

The theory of optimal control is used to determine the control law to accomplish an assigned mission. The goal of the procedure is the minimization of the trip time t_f; the problem is changed into a maximization problem by introducing the performance index $\phi = -t_f$.

An adjoint variable is associated with each state variable and the Hamiltonian is defined as

$$H = \lambda_r u + \lambda_\theta v/r + \lambda_u(v^2/r - 1/r^2) - \lambda_v uv/r + a_c/(2r^2)\cos\alpha[\lambda_u(1+\eta\cos 2\alpha) + \lambda_v\eta\sin 2\alpha] \tag{7}$$

The derivative of the adjoint variable which is associated with a generic variable x is provided by the Euler–Lagrange equation

$$\dot{\lambda}_x = -\frac{\partial H}{\partial x} \tag{8}$$

The full set of adjoint equations is omitted for the sake of conciseness. The application of the theory of optimal control produces a boundary value problem (BVP) for the state and adjoint variables. The BVP, which is presented in the following, is solved by means of a numerical procedure based on Newton's method (see Ref. 9). Tentative values are assumed for the unknown parameters and are progressively corrected to satisfy the prescribed boundary conditions.

Optimal Control Law

Pontriagyn's maximum principle states that the optimal control maximizes H over the set of admissible values. The adjoint variables λ_u and λ_v are the radial and tangential components, respectively, of the primer vector[10] $\boldsymbol{\lambda}_V$, which is the adjoint vector associated with the velocity vector. By introducing the angle β between $\boldsymbol{\lambda}_V$ and the radial direction [where β ranges from -180 to 180 deg and is positive according to the same rule as for α (Fig. 1)], one obtains $\lambda_u = \lambda_V\cos\beta$ and $\lambda_v = \lambda_V\sin\beta$, and the Hamiltonian is rewritten as

$$H = \lambda_r u + \lambda_\theta v/r + \lambda_u(v^2/r - 1/r^2) - \lambda_v uv/r + a_c\lambda_V/(2r^2)\cos\alpha[\cos\beta(1+\eta\cos 2\alpha) + \eta\sin\beta\sin 2\alpha] \tag{9}$$

The maximization of H with respect to the control variable α is equivalently accomplished by maximizing the simpler function:

$$H'(\alpha) = \cos\alpha[\cos\beta(1+\eta\cos 2\alpha) + \eta\sin\beta\sin 2\alpha] \tag{10}$$

The angle α that maximizes H' must have the same sign of β because $H'(\alpha) - H'(-\alpha) = 2\eta\cos\alpha\sin\beta\sin 2\alpha$ would be negative in the opposite case. Figure 2 shows the typical behavior of H' for different values of β (not to the same scale); positive values of α and β are

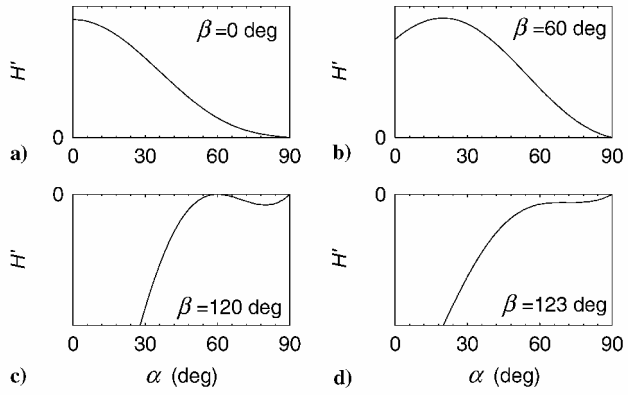

Fig. 2 Typical behaviors of the function H' for $\eta = 0.5$.

considered because $H'(\alpha, \beta) = H'(-\alpha, -\beta)$.

After Eq. (10) is rewritten as

$$H' = \cos\alpha[\cos\beta + \eta\cos(\beta - 2\alpha)] \tag{11}$$

the local maximum of H' is found by nullifying its partial derivative with respect to α. One obtains

$$-\sin\alpha[\cos\beta + \eta\cos(\beta - 2\alpha)] + 2\eta\cos\alpha\sin(\beta - 2\alpha) = 0 \tag{12}$$

By recognizing that

$$\sin(\beta - \alpha) = \sin[\alpha + (\beta - 2\alpha)]$$

$$= \cos\alpha\sin(\beta - 2\alpha) + \sin\alpha\cos(\beta - 2\alpha) \tag{13}$$

one obtains

$$-\sin\alpha\cos(\beta - 2\alpha) = \cos\alpha\sin(\beta - 2\alpha)$$

$$-\cos\alpha\sin\beta + \sin\alpha\cos\beta \tag{14}$$

which is substituted into Eq. (12) to provide, eventually,

$$\sin(\beta - 2\alpha) = [\sin\beta + (1 - \eta)/\eta\cos\beta\tan\alpha]/3 \tag{15}$$

Note that $H' = 0$ for $\alpha = \pm 90$ deg but that the local maximum corresponds to $H' < 0$ when β is sufficiently large (Fig. 2d). The limit value $\cos\beta = -\eta$ corresponding to a local maximum $H' = 0$ (Fig. 2c) is found by nullifying Eq. (10) and combining it with Eq. (15). The related sail orientation is $\alpha = \beta/2$. When $\cos\beta > -\eta$ (Figs. 2a and 2b), the optimal control is provided by the numerical solution of Eq. (15); Newton's method can, for instance, be adopted, when the solution that corresponds to $\eta = 1$ (i.e., ideal sail or unit reflectivity), that is, $\alpha = [\beta - \sin^{-1}(\frac{1}{3}\sin\beta)]/2$ is used as the starting guess. On the contrary, when $\cos\beta < -\eta$, then H' is maximized for $\alpha = 90$ deg, that is, the sail is edge-on with the radial direction and provides no thrust. Therefore, coast arcs may appear in the optimal trajectory of a nonideal solar sail. This important conclusion was first reached by Sauer[7] using a similar indirect approach.

Boundary Conditions

The problem is completed by the specification of the boundary conditions. Simple missions are considered to pay attention mainly to the aspects related to the sail characteristics. Circular orbits on the ecliptic plane are assumed for the planets. The boundary conditions corresponding to more complex cases may be found elsewhere.[11] At departure ($t_0 = 0$), the spacecraft leaves the Earth with zero hyperbolic excess velocity. The initial conditions for the state variables are $r_0 = 1$, $\theta_0 = 0$, $u_0 = 0$, and $v_0 = 1$.

The boundary conditions at the final point (subscript f) depend on the mission that is considered. When rendezvous with a planet is sought, the boundary conditions are $r_f = r_t$, $u_f = 0$, and $v_f = 1/\sqrt{r_t}$, where r_t is the radius of the planet's orbit. The departure time can be chosen to have the most suitable phase angle between the planets, and the final longitude θ_f is, therefore, left free. The time to reach a large assigned distance from the sun (in this paper 200 AU, according to previous works[12]) is minimized for the escape trajectory. The corresponding boundary condition is $r_f = 200$ AU. The theory of optimal control provides the additional boundary conditions to complete the differential problem.[13,14] One easily obtains $\lambda_{\theta f} = 0$ (rendezvous) and $\lambda_{\theta f} = \lambda_{uf} = \lambda_{vf} = 0$ (escape). The final time is minimized, and the transversality condition is $H_f = 1$ for both missions.

A spacecraft, which uses a solar sail to escape from the solar system, moves toward the sun, where a large thrust can be obtained, in the initial phase of the trajectory. When the characteristic acceleration is large enough, the spacecraft would pass extremely close to the sun, and it is advisable to impose a constraint on the minimum distance; in this paper $r_{\min} = 0.25$ AU has been chosen.[12] The trajectory is split into two arcs at the perihelion, where the constraints $r_p = r_{\min}$ and $u_p = 0$ are enforced. By applying the theory of optimal control, one easily finds that the radius adjoint variable can undergo a free jump in correspondence to the perihelion, where the other adjoint variables must be continuous; the jump $\Delta\lambda_r$ and t_p are two additional parameters whose values are determined by the optimization procedure to satisfy the additional conditions enforced at the perihelion.

Numerical Results

The optimal trajectory is determined when the sail reflectivity η and characteristic acceleration a_c are given. The latter also determines the payload fraction k_p when the sail areal density $\sigma = m_s/A$ is assigned. The total mass m is in fact the sum of the payload and the sail mass, which is proportional to the sail area via σ. Therefore,

$$k_p = 1 - \sigma A/m = 1 - \sigma a_c/(2p_1) \tag{16}$$

The characteristic acceleration cannot exceed the limit value $2p_1/\sigma$, which depends on the level of the sail technology and corresponds to a mission with zero payload.

The optimization procedure suggests a quasi-circular trajectory in the case of a planetary rendezvous mission. Figure 3 shows the flight time of a Mars mission as a function of the characteristic acceleration. In particular, the most interesting performance is obtained when the available thrust allows the spacecraft to reach the target after an integral number of revolutions around the sun. After each revolution, the spacecraft orbit is circularized to avoid the time-consuming passage through a distant aphelion where the thrust acceleration would be low for a long time. Figure 4 shows the control law for a two-revolution trajectory with $\eta = 0.8$. During each revolution, eccentricity and aphelion are first increased, whereas the perihelion is almost constant. The eccentricity is then reduced, and

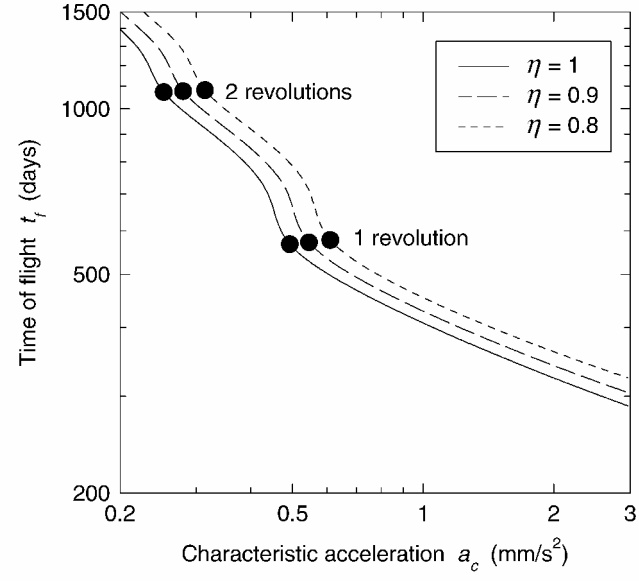

Fig. 3 Trip time of Mars rendezvous missions.

Table 1 Mars missions, 500 days

η	a_c, mm/s^2	ηa_c, mm/s^2	$k_p(\sigma = 10$ g/m$^2)$
1	0.6055	0.6055	0.3357
0.9	0.6831	0.6148	0.2505
0.8	0.7847	0.6278	0.1389

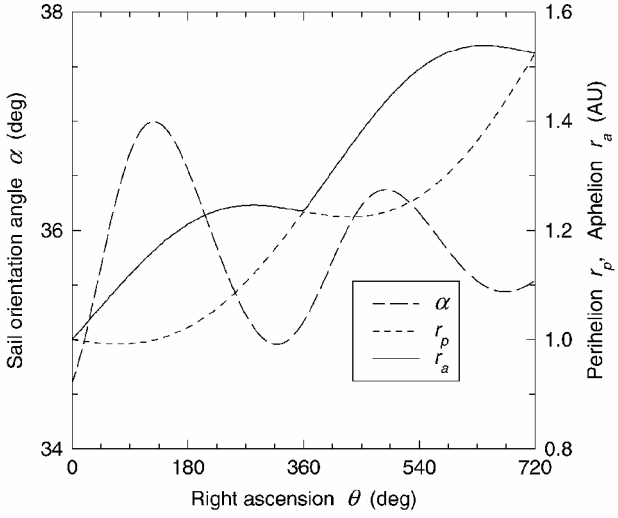

Fig. 4 Optimal control law for a 1080-day Mars mission, $\eta = 0.8$.

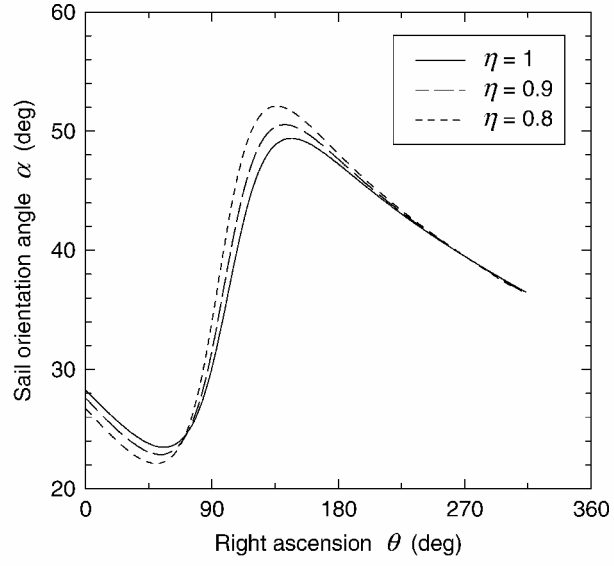

Fig. 5 Optimal control laws for 500-day Mars missions.

the perihelion is increased until the orbit is circularized. The process is reiterated in the subsequent revolution. The sail orientation angle is almost constant during this efficient maneuver, but the control history significantly differs when a nonintegral number of revolutions is performed. A wider range of orientation angles is exploited at short distances from the sun, where the sail is more effective.

A 500-day transfer to Mars, which constitutes a satisfactory compromise to contain both flight time and sail surface, has been the subject of a deeper analysis. The imperfect reflectivity of the sail must be offset by a higher characteristic acceleration, that is, by a larger sail area. Table 1 shows that the same trip time is obtained if the product ηa_c is almost constant, but a larger and less reflective sail penalizes the payload fraction. However, the sail technology that will probably be available in the near future ($\sigma = 10$ g/m^2) would provide a sufficient payload. The control laws for the corresponding missions are shown in Fig. 5. The range of the sail orientation angle is larger when the sail reflectivity is lower.

Figure 6, which refers to a Mercury rendezvous mission, shows the same oscillating trend of the flight time as in Fig. 3. The oscillations disappear when the maneuver is completed in less than one revolution. On the other hand, they are smoothed when a higher number of revolutions can more easily compensate for a nonzero phase angle between departure and arrival points. A 450-day mission is selected in this case. Two revolutions around the sun are completed before attaining the target because, in this case, the trajectory is closer to the sun. Table 2 shows that a Mercury rendezvous missions requires, like the Mars mission, a characteristic acceleration that is slightly more than proportional to the inverse of the sail reflectivity to obtain the same trip time as with the ideal sail. The same level of sail technology ($\sigma = 10$ g/m^2) also assures an adequate payload fraction in this case. Figure 7, which shows the optimal control

Table 2 Mercury missions, 450 days

η	a_c, mm/s^2	ηa_c, mm/s^2	$k_p(\sigma = 10$ g/m$^2)$
1	0.5398	0.5398	0.4077
0.9	0.6023	0.5421	0.3391
0.8	0.6817	0.5453	0.2520

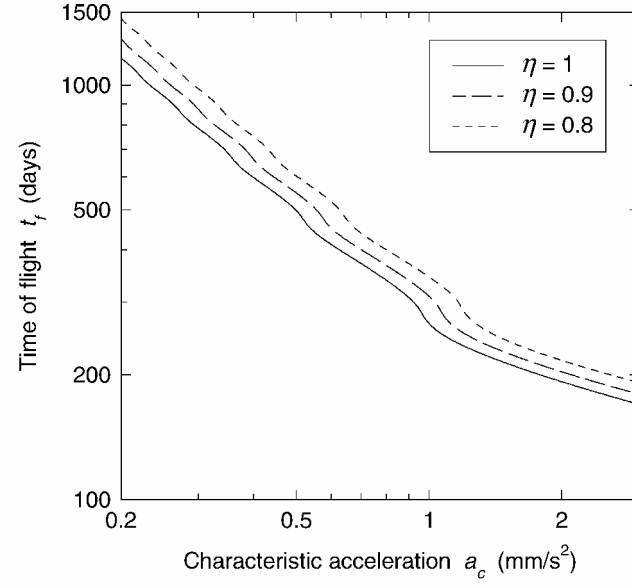

Fig. 6 Trip time of Mercury rendezvous missions.

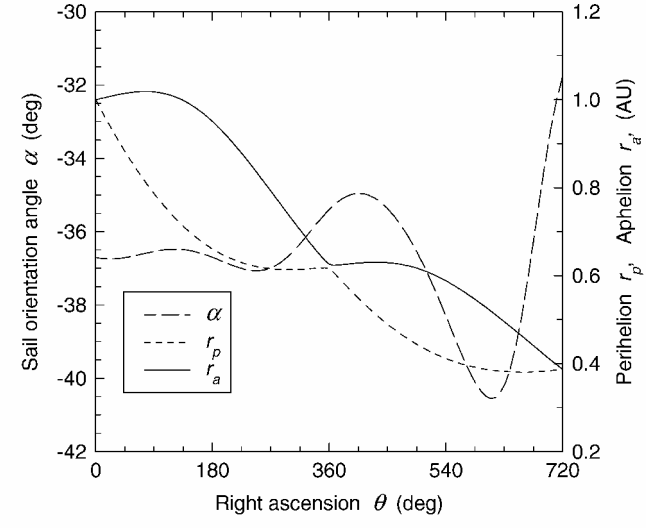

Fig. 7 Optimal control law for a 450-day Mercury mission, $\eta = 0.8$.

Table 3 Missions of 20 years to 200 AU

η	a_c, mm/s^2	ηa_c, mm/s^2	$k_p(\sigma = 3$ g/m$^2)$
1	1.7777	1.7777	0.4147
0.9	1.9385	1.7447	0.3619
0.8	2.1276	1.7021	0.2998

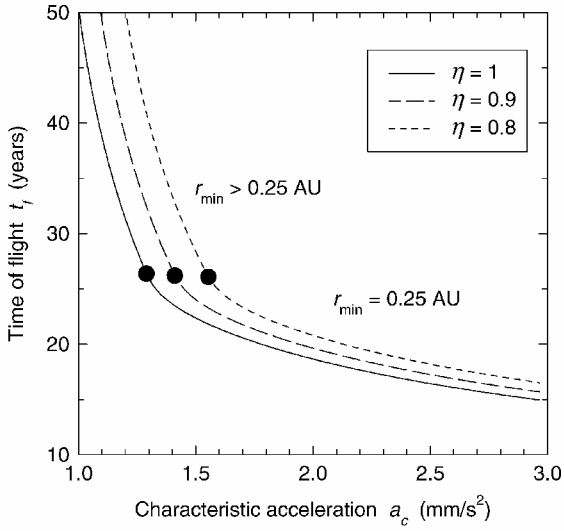

Fig. 8 Trip time to reach 200 AU.

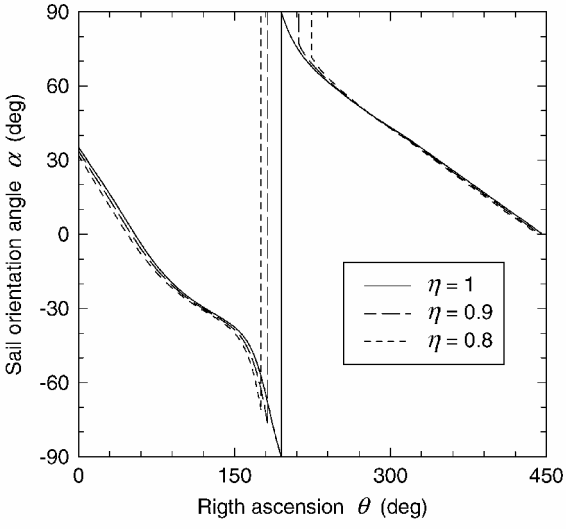

Fig. 9 Optimal control laws to reach 200 AU.

law for this two-revolution inbound mission, exhibits symmetrical features to the outbound mission described in Fig. 4.

An escape mission from the solar system has also been considered. Figure 8 presents the trip time to attain 200 AU, as a function of the characteristic acceleration and sail reflectivity. The spacecraft tends to move close to the sun to obtain a very large thrust from the high radiation flux. The constraint $r_{min} = 0.25$ AU is enforced and is active on the right of the symbols in Fig. 8. The maximum acceptable time to accomplish the mission is probably 20 years, and very high characteristic acceleration is necessary. The required a_c is, in this case, less than proportional to the inverse of the sail reflectivity (Table 3) because the radial component of the thrust is useful to accelerate the spacecraft, which moves almost radially after the perihelion of the trajectory. A sail areal density $\sigma = 3$ g/m^2, which implies a significant improvement of the current sail technology, is sufficient to carry an adequate payload. The control laws for different values of the sail reflectivity are shown in Fig. 9. An

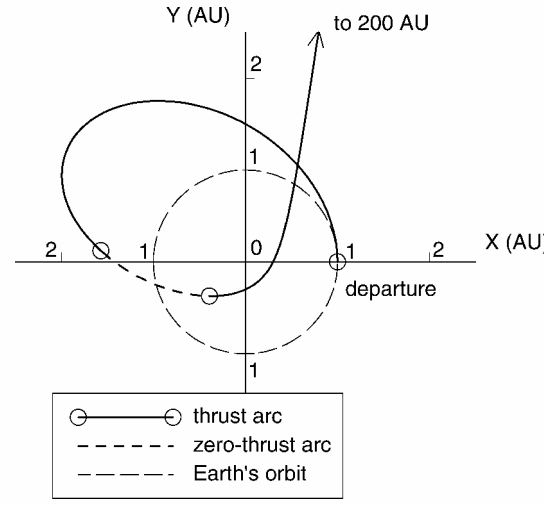

Fig. 10 Initial phase of the minimum-time trajectory to 200 AU, η = 0.8.

optimal escape trajectory is shown in Fig. 10, assuming $\eta = 0.8$. The spacecraft initially exploits the solar radiation pressure to reach an eccentric heliocentric orbit. The sail is then used to brake the spacecraft and lower the perihelion to the 0.25-AU limit. The surface of a sail, which is not perfectly reflective, is oriented parallel to the solar radiation for a short coast arc, while the spacecraft moves toward the sun (Figs. 9 and 10).

Conclusions

An indirect optimization procedure has been used to assess the performance of nonideal solar sails for interplanetary missions. The paper describes the application of the theory of optimal control and presents the analytical equation that defines the optimal orientation of the sail. The control laws of ideal and nonideal sails are quite similar, but real sails exhibit a wider range of orientation angles. Moreover, a perfectly reflective sail always exploits the solar pressure, whereas a partially reflective sail is feathered during particular phases of the mission, namely, when the spacecraft is moving fast toward the sun.

Missions toward inner and outer planets and escape trajectories have been considered to compare the performance of ideal and nonideal sails. All missions can be carried out with the same trip time as when using a unit-reflectivity sail, but a larger sail is necessary in the nonideal case, which leads to a penalty in terms of payload. The results of preliminary mission analyses assuming unit reflectivity can be used to estimate the performance of nonideal sails because, according to empirical evidence, the necessary surface area is practically proportional to the inverse of the sail reflectivity. Some significant features of the optimal trajectories have also been highlighted. In particular, the dependence of the trip time on the sail area is also affected by the trajectory geometry, and specific values of the characteristic acceleration are found to be more favorable for assigned mission and sail reflectivity.

References

[1] Forward, R. L., "Grey Solar Sails," *Journal of the Astronautical Sciences*, Vol. 38, No. 2, 1990, pp. 161–185.

[2] Sauer, C. G., Jr., "Optimum Solar-Sail Interplanetary Trajectories," AIAA Paper 76-0792, Aug. 1976.

[3] Wood, L. J., Bauer, T. P., and Zondervan, K. P., "Comment on 'Time-Optimal Orbit Transfer Trajectory for Solar Sail Spacecraft,'" *Journal of Guidance, Control, and Dynamics*, Vol. 5, No. 2, 1982, pp. 221–224.

[4] Subba Rao, P. V., and Ramanan, R. V., "Optimum Rendezvous Transfer Between Coplanar Heliocentric Elliptic Orbits Using Solar Sail," *Journal of Guidance, Control, and Dynamics*, Vol. 25, No. 6, 1992, pp. 1507–1509.

[5] Sauer, C. G., Jr., "Solar Sail Trajectories for Solar Polar and Interstellar Probe Missions," *Advances in Astronautical Sciences*, Vol. 103, Pt. 1, Univelt, Inc., San Diego, CA, 1999, pp. 547–562.

[6]McInnes, C. R., "Payload Mass Fractions for Minimum-Time Trajectories of Flat and Compound Solar Sails," *Journal of Guidance, Control, and Dynamics*, Vol. 23, No. 6, 2000, pp. 1076–1078.

[7]Sauer, C. G., Jr., "A Comparison of Solar Sail and Ion Drive Trajectories for a Halley's Comet Rendezvous Mission," American Astronautical Society, AAS Paper 77-104, Sept. 1977.

[8]Cichan, T., and Melton, R. G., "Optimal Trajectories for Non-Ideal Solar Sails," American Astronautical Society, AAS Paper 01-471, July–Aug. 2001.

[9]Colasurdo, G., and Pastrone, D., "Indirect Optimization Method for Impulsive Transfer," AIAA Paper 94-3762, Aug. 1994.

[10]Lawden, D. F., *Optimal Trajectories for Space Navigation*, Butterworths, London, 1963, pp. 54–68.

[11]Colasurdo, G., and Casalino, L., "Trajectories Towards Near-Earth-Objects Using Solar Electric Propulsion," *Advances in the Astronautical Sciences*, Vol. 103, Pt. 1, Univelt, Inc., San Diego, CA, 1999, pp. 593–607.

[12]Wallace, R. A., Ayon, J. A., and Sprague, G. A., "Interstellar Probe Mission/System Concept," *Journal of Space Mission Architecture*, No. 2, 2000, pp. 15–34.

[13]Bryson, A. E., and Ho, Y.-C., *Applied Optimal Control*, rev., Hemisphere, Washington, DC, 1975, pp. 106–108.

[14]Casalino, L., Colasurdo, G., and Pastrone, D., "Optimization Procedure for Preliminary Design of Opposition-Class Mars Missions," *Journal of Guidance, Control, and Dynamics*, Vol. 21, No. 1, 1998, pp. 134–140.

C. A. Kluever
Associate Editor